

# Dilute Bose gases interacting via power-law potentials

Ryan M. Kalas and D. Blume

*Department of Physics and Astronomy, Washington State University, Pullman, Washington 99164-2814*

Neutral atoms interact through a van der Waals potential which asymptotically falls off as  $r^{-6}$ . In ultracold gases, this interaction can be described to a good approximation by the atom-atom scattering length. However, corrections arise that depend on the characteristic length of the van der Waals potential. We parameterize these corrections by analyzing the energies of two- and few-atom systems under external harmonic confinement, obtained by numerically and analytically solving the Schrödinger equation. We generalize our results to particles interacting through a longer-ranged potential which asymptotically falls off as  $r^{-4}$ .

PACS numbers:

## I. INTRODUCTION

The interaction strengths of sufficiently dilute and cold bosonic atom samples such as Bose-Einstein condensates of alkali atoms can be parameterized to a good approximation by a single parameter, the  $s$ -wave scattering length [1]. In these systems, the neutral atoms interact through short-ranged van der Waals potentials which fall off as  $r^{-6}$  at large interparticle distances  $r$ . More recently, progress has been made in cooling and trapping systems characterized by interaction potentials that fall off more slowly than  $r^{-6}$  at large  $r$ . For example, the interaction between a neutral atom and an ion is dominated by a polarization potential that falls off asymptotically as  $r^{-4}$  [2]. Atom-ion systems have recently been proposed as candidates for quantum computing applications [3], and also play a role in recent work which proposes that macroscopic molecules can be formed by immersing an ion in a condensed Bose gas [4, 5, 6]. Another example for systems with longer-ranged interactions are dipolar gases [7, 8]. In these systems, the non-negligible magnetic or electric dipole moment leads to an angle-dependent  $r^{-3}$  potential at large interparticle distances. A natural question to ask is how well the properties of Bose systems with longer-ranged interactions can be described by the  $s$ -wave scattering length.

This paper considers dilute bosonic systems under external confinement interacting through spherically symmetric power-law potentials. In particular, we treat interactions with  $r^{-n}$  tails, where  $n$  is 4 or 6. We focus on the regime where the characteristic length  $\beta_n$  of the two-body potential is much smaller than the characteristic length  $a_{ho}$  of the trapping potential. In this regime, the shape-dependent interaction potential can be replaced by a regularized zero-range potential whose interaction strength is parametrized by the  $s$ -wave scattering length. For the potential with  $r^{-6}$  tail, e.g., it has been shown previously that the energy levels of the trapped two-body system can be reproduced very accurately if the energy-dependence of the scattering length is accounted for [9, 10]. This paper extends the two-body analysis to potentials with  $r^{-4}$  tail, whose scattering length has—because of the longer-ranged character of

the potential—a stronger energy-dependence than that of potentials with  $r^{-6}$  tail. We find that the corrections to the energy predicted by the zero-energy scattering length go as  $(\beta_6/a_{ho})^3$  and  $(\beta_4/a_{ho})^2$  for the interaction potentials with  $r^{-6}$  and  $r^{-4}$  tails, respectively.

Using Monte Carlo techniques, we furthermore treat dilute bosonic many-body systems. As in the two-body case, we consider different interaction potentials and analyze the resulting eigenenergies. Not unexpectedly, our results show that the energy-dependent scattering length remains a good quantity also in the many-body system. This suggests, e.g., that the description of dilute Bose gases within a mean-field Gross-Pitaevskii framework can be improved notably by including the energy-dependence of the scattering length. First steps in this direction have already been taken [6, 11]; our results provide additional benchmark results that may aid in further assessing the accuracy of these and related frameworks.

Section II introduces the Hamiltonian and the model interaction potentials used in our study. Section III discusses the energetics of two particles in a trap interacting through both finite-range and zero-range potentials. In Sec. IV, we consider the energetics of more than two particles in a trap by solving the many-body Schrödinger equation using Monte Carlo techniques. Finally, Sec. V concludes.

## II. HAMILTONIAN

The Hamiltonian for a system consisting of  $N$  identical mass  $m$  bosons in the presence of a spherically symmetric harmonic trapping potential with angular frequency  $\omega$  is given by

$$H = \sum_{i=1}^N \left( -\frac{\hbar^2}{2m} \nabla_i^2 + \frac{1}{2} m \omega^2 \mathbf{r}_i^2 \right) + \sum_{i<j}^N v(r_{ij}), \quad (1)$$

where  $\mathbf{r}_i$  denotes the position vector of the  $i$ th atom. The spherically symmetric two-body interaction potential  $v$  depends on the relative distance  $r_{ij}$ ,  $r_{ij} = |\mathbf{r}_i - \mathbf{r}_j|$ . We consider attractive power-law potentials with a hardcore

radius  $r_c$ ,

$$v_n(r) = \begin{cases} \infty & \text{for } r < r_c \\ -C_n/r^n & \text{for } r > r_c, \end{cases} \quad (2)$$

with  $n = 4, 6$  and  $C_n > 0$ . The Hamiltonian defined in Eq. (1) is characterized by three length scales: the hardcore radius  $r_c$ , the van der Waals length scale  $\beta_n$  [ $\beta_n = (mC_n/\hbar^2)^{1/(n-2)}$ ], and the harmonic oscillator length  $a_{ho}$  [ $a_{ho} = \sqrt{\hbar/m\omega}$ ]. Throughout this paper, we are interested in the regime where  $r_c$  and  $\beta_n$  are much smaller than  $a_{ho}$ .

In three dimensions, the interaction strength of any potential that falls off faster than  $r^{-3}$  at large distances can be characterized by the energy-dependent free-space  $s$ -wave scattering length  $a(k)$  [17],

$$a(k) = -\frac{\tan \delta(k)}{k}, \quad (3)$$

where  $\delta(k)$  denotes the  $s$ -wave scattering phase shift and  $k$  the wave vector at the scattering energy of  $\hbar^2 k^2/m$ . The zero-energy scattering length  $a(0)$  is defined by taking the  $k \rightarrow 0$  limit of Eq. (3). For the  $v_4$  and  $v_6$  potentials, the zero-energy and energy-dependent scattering lengths can be calculated from analytical solutions derived using series expansion techniques [12, 13].

Figures 1(a) and 2(a) show the zero-energy scattering length  $a(0)$  as a function of  $\beta_n$  for the  $v_n$  potential with  $r_c = 0.007a_{ho}$  for  $n$  equals 4 and 6, respectively. Although the scattering lengths are calculated for the free-space system with no external trapping potential, we choose to express all lengths in units of  $a_{ho}$  to ease the comparison with the trapped system in Secs. III and IV. When  $\beta_n = 0$ , the scattering length coincides with the hardcore radius  $r_c$ . As  $\beta_n$  increases, the attractive tails of the  $v_n$  potentials increase in strengths, which leads to a decrease of the scattering lengths. This continues until the potential is strong enough to support its first bound state, at which point the scattering length changes its sign from negative to positive. Figures 1(a) and 2(a) indicate that this divergence occurs at different values of  $\beta_n$ , i.e., at  $\beta_4 \approx 0.022a_{ho}$  and  $\beta_6 \approx 0.016a_{ho}$ , owing to the fact that the  $v_6$  potential is shorter-ranged than the  $v_4$  potential. This can be understood heuristically by considering the ratio of the attractive power of the potentials, that is, the ratio  $\int v_6(r)d^3\mathbf{r} / \int v_4(r)d^3\mathbf{r}$ . Taking the limits of the  $r$ -integration as  $r_c$  and  $\infty$ , this ratio equals  $\beta_6^4/(3\beta_4^2 r_c^2)$ . Looking at equal values of  $\beta_4$  and  $\beta_6$  and considering that  $\beta_n > r_c$  at the first divergence, this ratio is greater than one, in agreement with the observation that the  $v_6$  potential supports an  $s$ -wave bound state for smaller values of  $\beta_n/a_{ho}$  than the  $v_4$  potential.

Throughout this paper we are interested in describing dilute Bose systems which interact primarily through binary  $s$ -wave collisions. In such systems, the short-range details of the interaction potential are not being probed, and the regularized zero-range pseudopotential

$v_{ps}(r)$  [14],

$$v_{ps}(r) = \frac{4\pi\hbar^2}{m} g \delta^{(3)}(\mathbf{r}) \frac{\partial}{\partial r} r, \quad (4)$$

reproduces many observables obtained for the true shape-dependent interaction potential—in our case, the  $v_4$  or  $v_6$  potential—accurately if the strength  $g$  is chosen properly. In Secs. III and IV we take  $g$  to be the zero-energy scattering length  $a(0)$  and the energy-dependent scattering length  $a(k)$  of the shape-dependent interaction potential  $v_n$ .

For two particles in a harmonic trap interacting through  $v_{ps}$ , the Schrödinger equation can be solved analytically [15]. The center of mass energy equals  $(n_{cm} + 3/2)\hbar\omega$  ( $n_{cm} = 0, 1, \dots$ ), and the  $s$ -wave eigenenergies  $E_{rel} = \varepsilon\hbar\omega$  of the Schrödinger equation in the relative coordinate are determined by [15]

$$\frac{g}{a_{ho}} = \frac{\Gamma(-\frac{\varepsilon}{2} + \frac{1}{4})}{\sqrt{2}\Gamma(-\frac{\varepsilon}{2} + \frac{3}{4})}. \quad (5)$$

The transcendental equation (5) can be solved straightforwardly for any given  $g$  using standard root-finding procedures. For  $N > 2$ , analytical solutions to the Schrödinger equation for trapped atoms interacting through  $v_{ps}$  are in general not known, and we instead resort to numerical techniques (see Sec. IV).

### III. TWO PARTICLES IN A TRAP

We first consider the Hamiltonian given in Eq. (1) with  $v = v_n$  for  $N = 2$ . After separating off the center of mass motion, we are left with a Schrödinger equation in the relative coordinate. We solve the corresponding one-dimensional differential equation numerically using  $B$ -splines. Figures 1(b) and 2(b) show the resulting relative  $s$ -wave eigenenergies, denoted by  $\varepsilon_{v_4}$  and  $\varepsilon_{v_6}$ , respectively, as a function of  $\beta_n$ . As in Figs. 1(a) and 2(a), the hardcore radius is fixed at  $r_c = 0.007a_{ho}$ . For those  $\beta_n$  values for which  $a(0)$  is small [see Figs. 1(a) and 2(a)], the eigenenergies  $\varepsilon_{v_n}$  coincide approximately with the eigenenergies  $(2n_{rel} + 3/2)$  of the non-interacting system, where  $n_{rel} = 0, 1, \dots$ . However, each time  $a(0)$  diverges, a new molecular state appears and the energy of the gas-like state decreases by approximately  $2\hbar\omega$ .

Next, we consider two trapped particles interacting through  $v_{ps}$ . We find that the zero-range pseudopotential with energy-dependent scattering length reproduces the eigenenergies  $\varepsilon_{v_n}$  for the shape-dependent potential  $v_n$  with high accuracy for all interaction strengths considered in Figs. 1 and 2. To obtain the eigenenergies for  $v_{ps}$  with  $g = a(k)$ , which we denote by  $\varepsilon_{a(\varepsilon)}$ , we calculate  $a(k)$  for different  $\beta_n$  and solve Eq. (5) self-consistently [9, 10], i.e., we require that  $\varepsilon\hbar\omega$  on the right-hand side of Eq. (5) agrees with the energy  $\hbar^2 k^2/m$  at which the two particles collide. Since  $\varepsilon_{v_n}$  and  $\varepsilon_{a(\varepsilon)}$  coincide to many digits, Eq. (5) can be used to describe the physics of

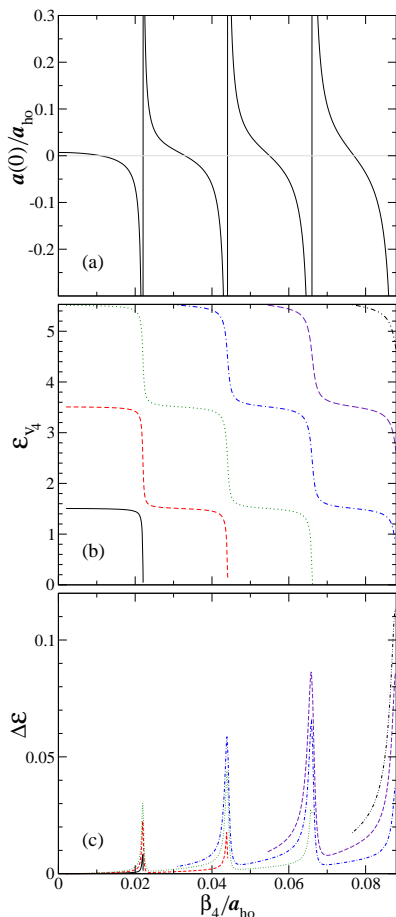


FIG. 1: (Color online)  $s$ -wave properties of two particles interacting through the potential  $v_4$  with  $r_c = 0.007a_{ho}$  as a function of  $\beta_4/a_{ho}$  (note that the  $x$ -axis is the same for all three panels): (a) Free-space zero-energy scattering length  $a(0)$ . (b) Relative energy  $\varepsilon_{v_4}$  for two trapped atoms. (c) Energy difference  $\Delta\varepsilon$ ,  $\Delta\varepsilon = \varepsilon_{v_4} - \varepsilon_{a(0)}$ , for two trapped atoms. In (b) and (c), the line styles are keyed to each other for ease of comparison.

two trapped particles provided  $\beta_n \ll a_{ho}$  and provided the energy-dependence of the scattering length is known. For short-range potentials, this was already shown in Refs. [9, 10]. For some systems under experimental study, only  $a(0)$  is known [ $a(k)$  is unknown]. It is thus useful to quantify the deviations  $\Delta\varepsilon$  between the eigenenergies  $\varepsilon_{v_n}$  and the eigenenergies  $\varepsilon_{a(0)}$  obtained from Eq. (5) with  $g = a(0)$ .

Figures 1(c) and 2(c) show the energy difference  $\Delta\varepsilon$ ,  $\Delta\varepsilon = \varepsilon_{v_n} - \varepsilon_{a(0)}$ , for the three energetically lowest-lying gas-like states. The line styles in Figs. 1(c) and 2(c) correspond to those used in Figs. 1(b) and 2(b). The energy difference  $\Delta\varepsilon$  is larger for the energetically higher-lying gas-like states since the energy-dependence of  $a(k)$  for a given  $\beta_n$  increases with increasing  $\varepsilon$ . The maximum of  $\Delta\varepsilon$  increases with increasing  $\beta_n/a_{ho}$  [see Fig. 1(c) and the inset of Fig. 2(c)] and is of the same order of magnitude for the  $v_4$  and  $v_6$  potentials for comparable values of

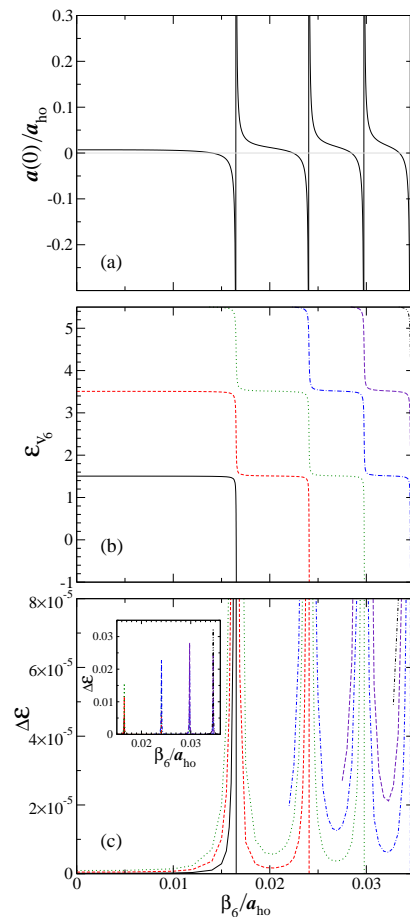


FIG. 2: (Color online)  $s$ -wave properties of two particles interacting through the potential  $v_6$  with  $r_c = 0.007a_{ho}$  as a function of  $\beta_6/a_{ho}$  (note that the  $x$ -axis is the same for all three panels): (a) Free-space zero-energy scattering length  $a(0)$ . (b) Relative energy  $\varepsilon_{v_6}$  for two trapped atoms. (c) Energy difference  $\Delta\varepsilon$ ,  $\Delta\varepsilon = \varepsilon_{v_6} - \varepsilon_{a(0)}$ , for two trapped atoms. The inset of (c) plots  $\Delta\varepsilon$  on an enlarged scale to show the maximum of  $\Delta\varepsilon$ . In (b) and (c), the lines styles are keyed to each other for ease of comparison.

$\beta_n/a_{ho}$ . Furthermore, for those  $\beta_n$  values for which the scattering length  $a(0)$  is comparatively small, the energy difference  $\Delta\varepsilon$  also increases with increasing  $\beta_n/a_{ho}$ . The magnitude of these “background” energy differences is much larger for the  $v_4$  potential than for the  $v_6$  potential [note the difference in the  $y$ -scales of Figs. 1(c) and 2(c)]. For example, for  $\beta_n \approx 0.03a_{ho}$ , the background energy is about  $10^{-3}\hbar\omega$  and  $10^{-5}\hbar\omega$  for the lowest-lying gas-like states of the  $v_4$  and  $v_6$  potentials, respectively. We now show that the background energy difference  $\Delta\varepsilon$  is proportional to  $(\beta_4/a_{ho})^2$  and  $(\beta_6/a_{ho})^3$  for the  $v_4$  and  $v_6$  potentials, respectively, thus explaining the much smaller energy difference for the  $v_6$  potential than for the  $v_4$  potential.

To arrive at these estimates, we use that  $\varepsilon_{a(\varepsilon)}$  agrees to many digits with  $\varepsilon_{v_n}$ , which implies  $\Delta\varepsilon = \varepsilon_{a(\varepsilon)} - \varepsilon_{a(0)}$ . Since  $\varepsilon_{a(\varepsilon)}$  is determined from Eq. (5) with  $g = a(\varepsilon)$ , we

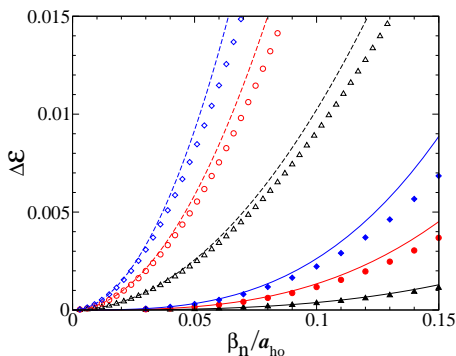


FIG. 3: (Color online) Energy difference  $\Delta\varepsilon$ ,  $\Delta\varepsilon = \varepsilon_{v_n} - \varepsilon_{a(0)}$ , for the three energetically lowest-lying gas-like states of two trapped atoms for  $a(0) = 0$  as a function of  $\beta_n/a_{ho}$ . The filled (open) triangles, circles and diamonds show the numerically determined energy differences for the levels near  $1.5$ ,  $3.5$  and  $5.5\hbar\omega$ , respectively, for the  $v_6$  ( $v_4$ ) potential. The solid and dashed lines show the corresponding analytically determined estimates for  $\Delta\varepsilon$ , Eqs. (13) and (12).

can obtain a simple expression for  $\varepsilon_{a(\varepsilon)}$  by expanding the left-hand side of Eq. (5) about  $a(0)$  and the right-hand side about  $\varepsilon_{a(0)}$ . The expansions of  $a(k)$  for the  $v_4$  and the  $v_6$  potential are given by [16]

$$a(k) = a(0) + \frac{\pi}{3}\beta_4^2 k + \dots \quad (6)$$

and [17]

$$a(k) = a(0) \left( 1 + \frac{1}{2}r_e a(0)k^2 + \dots \right), \quad (7)$$

respectively. In Eq. (7),  $r_e$  denotes the effective range of the  $v_6$  potential [11, 18],

$$\frac{r_e}{\beta_6} = \frac{2}{3x_e} \frac{1}{(a(0)/\beta_6)^2} \left[ 1 + \left( 1 - x_e \frac{a(0)}{\beta_6} \right)^2 \right], \quad (8)$$

where the constant  $x_e = [\Gamma(1/4)]^2/(2\pi) \approx 2.09$ . Denoting the right-hand side of Eq. (5) by  $f(\varepsilon_{a(0)})$  for  $g = a(0)$ , we find

$$\Delta\varepsilon \approx \frac{\frac{\pi}{3} \left( \frac{\beta_4}{a_{ho}} \right)^2 \sqrt{\varepsilon_{a(0)}}}{f'(\varepsilon_{a(0)}) - \frac{\pi}{3} \left( \frac{\beta_4}{a_{ho}} \right)^2 \sqrt{\varepsilon_{a(0)}}} \quad (9)$$

for the  $v_4$  potential and

$$\Delta\varepsilon \approx \frac{\frac{1}{2} \frac{r_e}{a_{ho}} \left( \frac{a(0)}{a_{ho}} \right)^2 \varepsilon_{a(0)}}{f'(\varepsilon_{a(0)}) - \frac{1}{2} \frac{r_e}{a_{ho}} \left( \frac{a(0)}{a_{ho}} \right)^2 \varepsilon_{a(0)}} \quad (10)$$

for the  $v_6$  potential. The different powers of  $\varepsilon_{a(0)}$  in Eqs. (9) and (10) follow directly from the linear and quadratic  $k$ -dependence of the correction terms in Eqs. (6) and (7), respectively.

If  $a(0) \ll \beta_6$ , the square bracket in the expression for the effective range  $r_e$  is approximately equal to 2 and

Eq. (10) reduces to

$$\Delta\varepsilon \approx \frac{\frac{2}{3x_e} \left( \frac{\beta_6}{a_{ho}} \right)^3 \varepsilon_{a(0)}}{f'(\varepsilon_{a(0)}) - \frac{2}{3x_e} \left( \frac{\beta_6}{a_{ho}} \right)^3 \varepsilon_{a(0)}}. \quad (11)$$

Furthermore, for small  $a(0)$ ,  $\varepsilon_{a(0)}$  is approximately given by  $(3/2 + 2n_{rel})$  and  $f'(\varepsilon_{a(0)})$  is of order 1 (taking values of approximately 1.25, 0.84, and 0.67 for  $n_{rel} = 0, 1$ , and 2). The second term in the denominator of Eqs. (9) and (11) can thus be dropped provided  $\beta_n$  is much smaller than  $a_{ho}$ . This yields

$$\Delta\varepsilon \approx \frac{\pi \sqrt{2n_{rel} + 3/2}}{3f'(2n_{rel} + 3/2)} \left( \frac{\beta_4}{a_{ho}} \right)^2 \quad (12)$$

for the  $v_4$  potential and

$$\Delta\varepsilon \approx \frac{2(2n_{rel} + 3/2)}{3x_e f'(2n_{rel} + 3/2)} \left( \frac{\beta_6}{a_{ho}} \right)^3 \quad (13)$$

for the  $v_6$  potential. Equations (12) and (13) can also be derived by applying first order perturbation theory to the trapped two-body system interacting through a zero-range potential (see Sec. IV).

Solid and dotted lines in Fig. 3 show the energy differences  $\Delta\varepsilon$  predicted by Eqs. (13) and (12) for  $n_{rel} = 0, 1$  and 2 (from bottom to top) as a function of  $\beta_n/a_{ho}$  for the  $v_6$  and  $v_4$  potential, respectively. For comparison, filled and open symbols in Fig. 3 show the corresponding numerically determined energy differences  $\Delta\varepsilon$  for the three energetically lowest-lying gas-like states. To calculate these energy differences, we fix  $r_e$  and  $\beta_n$  so that  $a(0) = 0$ , and vary the harmonic oscillator length. We find that, as long as  $r_e$  and  $\beta_n \ll a_{ho}$ , the results shown in Fig. 3 are independent of the number of bound states supported by the shape-dependent power-law potential  $v_n$ . Figure 3 illustrates that the estimates given in Eqs. (12) and (13) are quite accurate for small  $a(0)$ . Thus, our derivation shows that the different powers of the characteristic length scale  $\beta_n$ , which explain the larger background values of  $\Delta\varepsilon$  for the  $v_4$  potential compared to the  $v_6$  potential, can be traced back to the different energy dependence of  $a(k)$  for the  $v_4$  and  $v_6$  potential.

#### IV. N PARTICLES IN A TRAP

To solve the time-independent Schrödinger equation for more than  $N = 2$  trapped particles, we resort to the variational Monte Carlo (VMC) and diffusion Monte Carlo (DMC) techniques [19].

In the VMC method, the variational many-body wave function  $\psi_V$  is written in terms of a set of variational parameters  $\mathbf{p}$ , which are optimized so as to minimize the variational energy  $E_V$ ,  $E_V = \langle \psi_V | H | \psi_V \rangle / \langle \psi_V | \psi_V \rangle$ . The energy expectation value  $E_V$  is calculated for a given  $\mathbf{p}$  using Metropolis sampling. Motivated by the structure of the Hamiltonian  $H$ , Eq. (1), we write  $\psi_V$  as a product

of one-body terms  $\varphi$  and two-body Jastrow terms  $F$  [20, 21, 22],

$$\psi_V(\mathbf{r}_1, \dots, \mathbf{r}_N) = \prod_{i=1}^N \varphi(r_i) \prod_{i<j}^N F(r_{ij}), \quad (14)$$

where  $\varphi(r) = \exp(-p_1 r^{p_2})$ . The functional form of the two-body Jastrow factor  $F$  is motivated by the functional form of the interaction potential  $v$  and by the fact that we are interested in describing the energetically lowest-lying gas-like state of the many-body Hamiltonian. We use

$$F(r) = \begin{cases} (1 - b/r)(1 + p_3/r^{p_4}) & \text{for } r > b \\ 0 & \text{for } r \leq b \end{cases} \quad (15)$$

for  $v = v_n$ , and

$$F(r) = \begin{cases} 0 & \text{for } r \leq c \\ \sin(kr + d) & \text{for } c < r \leq p_5 \\ e_1 + e_2 \exp(-p_6 r) & \text{for } r > p_5 \end{cases} \quad (16)$$

for  $v = v_{ps}$ . The parameters  $b$ ,  $c$ ,  $d$  and  $k$  are chosen so that  $\psi_V$  obeys the boundary conditions implied by the many-body Hamiltonian  $H$  and so that  $\psi_V$  has the desired symmetry (see below), while the parameters  $e_1$  and  $e_2$  are determined by requiring that  $F$  and its derivative are continuous at  $r = p_5$ . For each interaction potential  $v$ , we optimize the variational parameters  $\mathbf{p}$ , i.e.,  $p_1$  through  $p_4$  for  $v = v_n$ , and  $p_1$ ,  $p_2$ ,  $p_5$  and  $p_6$  for  $v = v_{ps}$ .

To go beyond the variational calculations, we apply two different variants of the DMC algorithm both of which use the optimized wave function  $\psi_V$  as a guiding function [19]. When the many-body Hamiltonian does not support any states with negative energy, the lowest lying gas-like state coincides with the true ground state of the system. In this case,  $\psi_V$  is nodeless and the DMC algorithm with importance sampling results in the exact many-body energy. When the many-body Hamiltonian supports negative energy states, i.e., molecular-like bound states, the energetically lowest lying gas-like state possesses nodes, which are imposed in the DMC method with importance sampling through the variational wave function  $\psi_V$ . This DMC variant, referred to as fixed-node DMC method [19, 23], determines the lowest energy of a state that has the same symmetry as  $\psi_V$ . Importantly, the FN-DMC energy provides an upper bound to the exact eigenenergy of the excited gas-like state of the many-body system [23].

The solid squares, triangles and diamonds in Fig. 4 show the total energy  $E_{v_4}(N)$  calculated by the DMC method for  $N = 4$  trapped particles interacting through the  $v_4$  potential with  $r_c = 0.007a_{ho}$  as a function of the zero-energy scattering length  $a(0)$  for a varying number of two-body  $s$ -wave bound states. The solid squares show energies for two-body potentials that support no  $s$ -wave bound state. For the two-body potentials considered, the corresponding four-body system supports no state

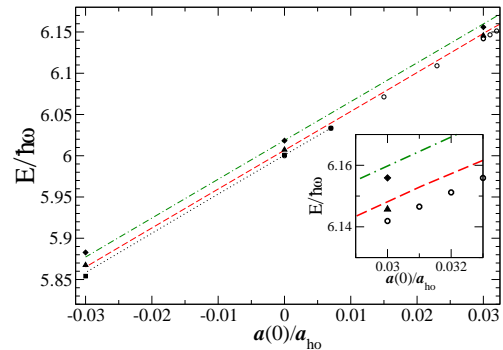


FIG. 4: (Color online) Solid squares, triangles and diamonds show the total energy  $E_{v_4}(N)$  calculated by the DMC method for four trapped particles interacting through the  $v_4$  potential with  $r_c = 0.007a_{ho}$  as a function of  $a(0)/a_{ho}$ . The dotted, dashed, and dash-dotted lines show the perturbative energies, Eq. (17), for two-body potentials that support 0, 1 and 2 bound states. Open circles show the total energy  $E_{a(0)}(N)$  calculated by the DMC method for four particles interacting through the zero-range pseudo-potential  $v_{ps}$  with  $g = a(0)$ . For all cases, the error bars of the energies are smaller than the symbol size. The inset shows an enlargement of the region around  $a(0) = 0.03a_{ho}$ .

with negative energy, and the hardcore boundary condition implied by  $v_4$  is met by setting the parameter  $b$  in Eq. (15) equal to  $r_c$ . The energies for those  $v_4$  potentials that support one and two  $s$ -wave bound states are shown by solid triangles and diamonds, respectively. In these cases, the four-particle system supports negative energy states, and the parameter  $b$  is chosen to coincide with the  $r$  value at which the free-space zero-energy two-body scattering solution has its first and second node, respectively. This construction of the many-body nodal surface assumes that at most two particles scatter at any given time, and that the nodal line of the two-body scattering solution is not modified by the presence of the other atoms [24, 25]. This “binary approximation” is expected to be quite accurate in the low-density regime considered throughout this paper. Figure 4 shows that, for a given zero-energy scattering length  $a(0)$ , the energy  $E_{v_4}$  of the lowest-lying gas-like state increases as the number of two-body  $s$ -wave bound states, or equivalently  $\beta_4/a_{ho}$ , increases, similar to the behavior found in Sec. II for the two particle case [see Fig. 1(c)].

For comparison, we consider the energy of  $N$  particles interacting through an energy-dependent zero-range pseudopotential, within first order perturbation theory,

$$\frac{E(N)}{\hbar\omega} = \frac{3}{2}N + \frac{N(N-1)}{2} \sqrt{\frac{2}{\pi}} \frac{a(k)}{a_{ho}}. \quad (17)$$

For weakly interacting systems, i.e., for small scattering lengths,  $a(k)$  can be approximated by Eq. (6) with  $k$  corresponding to the trap energy scale of  $3/2\hbar\omega$ . The perturbative results for  $N = 4$  particles are shown in

Fig. 4 by dotted, dashed and dash-dotted lines for the cases when the two-body potential supports zero, one and two bound states. The agreement between the perturbative and DMC energies is reasonably good over the range of scattering lengths considered. In particular, the perturbative expression with the energy-dependent scattering length predicts the up-shift of the energies with increasing number of two-body bound states for a fixed  $a(0)$  correctly but does not fully capture the change of slope of the energy with increasing  $|a(0)|$ .

Next we consider the DMC results for  $N$  trapped atoms interacting through the pseudo-potential  $v_{ps}$  with  $g = a(0)$ . The potential  $v_{ps}$  possesses one bound state for  $g > 0$  and no bound state for  $g < 0$ . For positive scattering lengths, we use the nodal surface of the free-space two-body scattering solution for  $v_{ps}$  to determine the parameters of the Jastrow factor  $F$ , Eq. (16), i.e., we use  $c = a(0)$  and  $d = \delta(k)$  with a very small  $k$  value. In addition to positive  $a(0)$ , we consider negative  $a(0)$ . Using  $\psi_V$  with  $c$ ,  $d$  and  $k$  chosen so that the boundary condition implied by the zero-range pseudo-potential is satisfied whenever one of the interparticle distances  $r_{ij}$  is zero, numerical instabilities associated with large negative DMC energies arise. These instabilities are most likely associated with the Thomas collapse [26, 27], which is known to occur for systems with three or more particles interacting through  $v_{ps}$  with  $g < 0$ .

The open circles in Fig. 4 show the total DMC energy  $E_{a(0)}(4)$  as a function of the zero-energy scattering length  $a(0)$  for  $a(0) \geq 0$ . We find that  $E_{a(0)}(4)$  is smaller than or equal to  $E_{v_4}(4)$  for all  $a(0)$ . To quantify to which extent the Hamiltonian with the shape-independent potential reproduces the properties of the Hamiltonian with the shape-dependent potential, we consider the energy difference  $\Delta E(N)$ ,  $\Delta E(N) = E_{v_4}(N) - E_{a(0)}(N)$ . For  $N = 4$  and 10, we find that  $\Delta E$  scales—as might be expected for a weakly-interacting Bose gas—with the number of pairs, i.e.,  $\Delta E(N)/\hbar\omega \approx N_{pair}\Delta\varepsilon_{v_4}$ , where  $\Delta\varepsilon_{v_4}$  denotes the energy difference introduced in Sec. III and  $N_{pair}$  the number of pairs,  $N_{pair} = N(N-1)/2$ . For  $N = 4$  and  $a(0) = 0.03a_{ho}$ , e.g., we find  $E_{v_4} = 6.1457(2)\hbar\omega$  (triangles in the inset of Fig. 4) for the  $v_4$  potential that supports one two-body  $s$ -wave bound state and  $E_{a(0)} = 6.14189(3)\hbar\omega$  (open circles in the inset of Fig. 4) for the zero-range potential with  $g = a(0)$ , and thus  $\Delta E = 0.0038(2)\hbar\omega$ . For comparison, the corresponding quantity  $N_{pair}\Delta\varepsilon$  equals  $0.0040\hbar\omega$ . In addition to the  $v_4$  potential, we consider the  $v_6$  potential. In this case, the energy difference  $\Delta E$  for comparatively small  $a(0)$  is of the same order or larger than the statistical uncertainties of our DMC energies and, although expected to be valid, we cannot explicitly confirm the scaling of  $\Delta E$  with  $N_{pair}$  for the  $v_6$  potential.

To further understand the implications of the energy-dependent scattering length  $a(E)$  for  $N > 2$ , we determine the  $a(E)$  that, if used to parametrize the interaction strength of the zero-range potential in the many-body Hamiltonian, reproduces the energy  $E_{v_4}$ . For example, to reproduce the four-particle energy  $E_{v_4} = 6.1457(2)$  for the  $v_4$  potential with  $a(0) = 0.03a_{ho}$  that supports one bound state, the strength of the pseudopotential has to be  $a(E) = 0.03082(4)$ . For the  $v_4$  potential, this  $a(E)$  corresponds to a two-body scattering energy of  $1.53(16)\hbar\omega$ . Thus, the relevant scattering energy for two-body collisions occurring in the weakly-interacting many-body is, not unexpectedly, approximately given by the trap energy scale of  $3/2\hbar\omega$ .

## V. CONCLUSION

This paper studies trapped bosons interacting through attractive power-law potentials with  $r^{-4}$  and  $r^{-6}$  tails. For two particles, the energy-dependent pseudo-potential accurately reproduces the energies for both shape-dependent potentials. Further, we find that the deviations between the energies obtained for the energy-independent pseudo-potential and the shape-dependent potential scale for small  $a(0)$  as  $(\beta_6/a_{ho})^3$  and  $(\beta_4/a_{ho})^2$  for the potentials with  $r^{-6}$  and  $r^{-4}$  tails, respectively. Finally, we use Monte Carlo methods to extend the treatment to more than two trapped particles. Again, we find that the energy for the shape-dependent power-law potential can be reproduced accurately by the energy-dependent pseudo-potential if the energy-scale entering the pseudo-potential is chosen properly. In general, this leads to a self-consistent many-body framework that considers only binary interactions but includes many-body correlations.

Even if the  $r^{-4}$  results are not directly applicable to present-day experiments (combined atom-ion systems have not yet been trapped), our comparative study of the energetics for  $r^{-4}$  and  $r^{-6}$  potentials provides insights into weakly interacting systems in general and van der Waals  $r^{-6}$  interactions in particular. Our calculations suggest that three-body terms [28] are very small in the dilute limit considered throughout this work. It seems feasible that the description of systems with longer-ranged interactions at the mean-field level can be improved by including the energy dependence of the scattering length, similar to the frameworks outlined in Refs. [6, 11].

We gratefully acknowledge support by the NSF through Grant No. PHY-0555316.

[1] C. J. Pethick and H. Smith, *Bose-Einstein Condensation in Dilute Gases* (Cambridge, 2001).

[2] B. H. Bransden and C. J. Joachain, *Physics of Atoms*

- and Molecules, 2nd ed.* (Prentice Hall, 2003).
- [3] Z. Idziaszek, T. Calarco, and P. Zoller, *Phys. Rev. A* **76**, 033409 (2007).
  - [4] R. Coté, V. Kharchenko, and M. D. Lukin, *Phys. Rev. Lett.* **89**, 093001 (2002).
  - [5] P. Massignan, C. J. Pethick, and H. Smith, *Phys. Rev. A* **71**, 023606 (2005).
  - [6] A. Collin, P. Massignan and C. J. Pethick, *Phys. Rev. A* **75**, 013615 (2007).
  - [7] L. Santos, G. V. Shlyapnikov, P. Zoller, and M. Lewenstein, *Phys. Rev. Lett.* **85**, 1791 (2000).
  - [8] A. Griesmaier, J. Werner, S. Hensler, J. Stuhler, and T. Pfau, *Phys. Rev. Lett.* **94**, 160401 (2005).
  - [9] D. Blume and C. H. Greene, *Phys. Rev. A* **65**, 043613 (2002).
  - [10] E. L. Bolda, E. Tiesinga, and P. S. Julienne, *Phys. Rev. A* **66**, 013403 (2002).
  - [11] H. Fu, Y. Wang, and B. Gao, *Phys. Rev. A* **67**, 053612 (2003).
  - [12] N. A. W. Holzwarth, *J. Math. Phys.* **14**, 191 (1973), and references therein.
  - [13] B. Gao, *Phys. Rev. A* **58**, 1728 (1998).
  - [14] K. Huang and C. N. Yang, *Phys. Rev.* **105**, 767 (1957).
  - [15] T. Busch, B.-G. Englert, K. Rzażewski, and M. Wilkens, *Found. Phys.* **28**, 549 (1998).
  - [16] T. F. O'Malley, L. Spruch, and L. Rosenberg, *J. Math. Phys.* **2**, 491 (1961). The next terms in the expansion of Eq. (6) are of order  $k^2$  and  $k^2 \ln(k\beta_4)$ .
  - [17] R. G. Newton, *Scattering Theory* (Dover, 2002).
  - [18] B. Gao, *Phys. Rev. A* **58**, 4222 (1998).
  - [19] B. L. Hammond, W. A. Lester, Jr., and P. J. Reynolds, *Monte Carlo Methods in Ab Initio Quantum Chemistry* (World Scientific, Singapore, 1994).
  - [20] R. Jastrow, *Phys. Rev.* **98**, 1479 (1955).
  - [21] J. L. DuBois and H. R. Glyde, *Phys. Rev. A* **63**, 023602 (2001).
  - [22] D. Blume and C. H. Greene, *Phys. Rev. A* **63**, 063601 (2001).
  - [23] P. J. Reynolds, D. M. Ceperley, B. J. Alder, and W. A. Lester, Jr., *J. Chem. Phys.* **77**, 5593 (1982).
  - [24] G. E. Astrakharchik, D. Blume, S. Giorgini, and B. E. Granger, *J Phys B* **37**, S205 (2004).
  - [25] I. Khan and B. Gao, *Phys. Rev. A* **73**, 063619 (2006).
  - [26] L.H. Thomas, *Phys. Rev.* **47**, 903 (1935).
  - [27] D. V. Fedorov and A. S. Jensen, *Phys. Rev. A* **63**, 063608 (2001).
  - [28] T. T. Wu, *Phys. Rev.* **115**, 1390 (1959).